Biosensors and Bioelectronics 183 (2021) 113204

Contents lists available at ScienceDirect

Biosensors and Bioelectronics

journal homepage: http://www.elsevier.com/locate/bios

Towards a flexible electrochemical biosensor fabricated from biocompatible *Bombyx mori* silk

Denise Molinnus [a], Aleksander Drinic [b], Heiko Iken [a], Nadja Kröger [c], Max Zinser [c], Ralf Smeets [d], Marius Köpf [b], Alexander Kopp [b], Michael J. Schöning [a,e,*]

[a] Institute of Nano- and Biotechnologies (INB), FH Aachen, Campus Jülich, Heinrich-Mußmann-Strasse 1, 52428, Jülich, Germany
[b] Fibrothelium GmbH, TRIWO Technopark Aachen, Philipsstr. 8, 52068, Aachen, Germany
[c] Department of Plastic, Reconstructive and Aesthetic Surgery, University Hospital of Cologne, Kerpener Str. 62, 50937, Cologne, Germany
[d] Department of Oral and Maxillofacial Surgery, Division of Regenerative Orofacial Medicine, University Medical Center Hamburg-Eppendorf, Martinistraße 52, Hamburg, Germany
[e] Forschungszentrum Jülich GmbH, Institute of Biological Information Processing (IBI-3), Wilhelm-Johnen-Strasse 6, 52425, Jülich, Germany

ARTICLE INFO

Keywords:
Silk fibroin
Flexible biosensor
Glucose
Biodegradable
Biocompatible

ABSTRACT

In modern days, there is an increasing relevance of and demand for flexible and biocompatible sensors for in-vivo and epidermal applications. One promising strategy is the implementation of biological (natural) polymers, which offer new opportunities for flexible biosensor devices due to their high biocompatibility and adjustable biodegradability. As a proof-of-concept experiment, a biosensor was fabricated by combining thin- (for Pt working- and counter electrode) and thick-film (for Ag/AgCl quasi-reference electrode) technologies: The biosensor consists of a fully bio-based and biodegradable fibroin substrate derived from silk fibroin of the silkworm *Bombyx mori* combined with immobilized enzyme glucose oxidase. The flexible glucose biosensor is encapsulated by a biocompatible silicon rubber which is certificated for a safe use onto human skin. Characterization of the sensor set-up is exemplarily demonstrated by glucose measurements in buffer and Ringer's solution, while the stability of the quasi-reference electrode has been investigated versus a commercial Ag/AgCl reference electrode. Repeated bending studies validated the mechanical properties of the electrode structures. The cross-sensitivity of the biosensor against ascorbic acid, noradrenaline and adrenaline was investigated, too. Additionally, biocompatibility and degradation tests of the silk fibroin with and without thin-film platinum electrodes were carried out.

1. Introduction

Biocompatible electronic devices are of particularly great interest with regard to biomedical applications and environmental monitoring (Onuki et al., 2008; Sajid et al., 2016). For example, implantable sensors play a key role in the realization of electric prosthetic hands (Weir et al., 2009) or to determine the pH value, concentrations of Na^+-, K^+-, Ca^{2+}-ions, glucose, lactate as well as the temperature in human blood (Arifuzzaman et al., 2019; Frost and Meyerhoff 2002; Kang et al., 2019; Kifle et al., 2019; Nouira et al., 2009; Pickup et al., 1987; Quinn et al., 1997; Rivnay et al., 2014; Vallejo-Heligon et al., 2016). For this, several materials such as polymers from natural origin (e.g., collagen, chitosan, alginate, hyaluronan, dextran, single cell thick onion membrane) (Cadée et al. 2001; Fujioka 1998; Geiger et al., 2003; Sajid et al., 2016; Vercruysse and Prestwich 1998; Vos et al., 2002) or synthetic polymers (Lunsford et al., 2000; Maruoka et al., 2006; Oka et al., 2000; Onuki et al., 2008; Paradossi et al., 2003) (poly(lactic acid) (PLA), poly (lactic-co-glycolic acid) (PLGA), poly(ethylene glycol) (PEG), 2-hydroxy ethyl methacrylate, or poly(vinyl alcohol) (PVA)) have been examined during the last years to be implemented into a variety of devices. Although these materials have been commonly used so far, there are, however, still some issues concerning their biocompatibility which impede the realization of implantable bioelectronic devices such as sensors or electrodes. In many cases, through the implantation of electronic devices based on biomaterials, there is still a risk of an inflammatory response caused by tissue injury or a 'classic' foreign body reaction (Anderson 2001; Anderson et al., 2008; Anderson and Langone 1999; Fournier et al., 2003; Onuki et al., 2008; Wang et al., 2015).

* Corresponding author. Institute of Nano- and Biotechnologies (INB), FH Aachen, Campus Jülich, Heinrich-Mußmann-Strasse 1, 52428, Jülich, Germany.
E-mail address: schoening@fh-aachen.de (M.J. Schöning).

https://doi.org/10.1016/j.bios.2021.113204
Received 17 December 2020; Received in revised form 22 March 2021; Accepted 24 March 2021
Available online 28 March 2021

In quest of excellent performance and reasonable costs for biomedical purposes, researchers are taking inspiration from nature as an alternative to conventional organic and inorganic materials. This opens up new possibilities to surpass expensive, synthetic materials: One strategy is the use of natural silk proteins as biomaterial, featuring beneficial properties such as high strength and elongation, pressure resistance as well as thermomechanical stability (Chen et al., 2012; Humenik et al., 2011; Kopp et al., 2019; Ude et al., 2014; Zhang et al., 2002). Silk proteins are extracted from cocoons which are produced by the domestic silk worm *Bombyx mori*, composed of two fibroin strands which are covered and separated by an outer sericin layer resulting in a silk thread with a diameter of about 10–25 μm. Due to its highly crystalline protein conformation, silk fibers are known as one of the strongest natural fibers making them a suitable alternative to synthetic fibers (Porter and Vollrath 2009; Sierra-Montes et al., 2005; Ude et al., 2014). Furthermore, the protein fibroin can be dissolved in aqueous solvents and then be transformed into various structures, like sponges, membranes, films, gels, powders, and scaffolds (Vepari and Kaplan 2007). Due to their diversity and remarkably high biocompatibility, silk proteins show an increasing potential in the production of green electronics used in food-sensing applications, improved physiological recording, targeted drug delivery and biomedical implants (Irimia-Vladu 2014). In addition, one of the major advantages of silk proteins is the biodegradability under physiological conditions driven by proteolytic enzymes (e.g., collagen, keratin, elastin). The degradation process is dependent on the architecture and morphology of the regenerated protein structure as well as of the type of enzymes being present (Arai et al., 2004; Lucas et al., 1957; Seves et al., 1998). For example, a porous sponge degrades more rapidly due to its high surface area, offering multiple interaction points for surface erosion, in comparison with a densely casted membrane (Cao and Wang 2009). Further, the degradation rate can be tailored, depending on the degree of crystallization of the recombined silk structure. The crystallinity describes the β-sheet content of the protein morphology, which can be raised by different methods, like treatment with organic solvent, temperature regulation, pH and mechanical stress (Rockwood et al., 2011). The degumming procedure, which is the necessary part of the protein isolation process, also influences the degradation behavior of the regenerated silk structures, depending on the degumming agent and the resulting molecular weight of the remaining protein (Wang et al., 2019).

Several examples for silk-based electronics have already been reported in literature such as a flexible organic thin-film transistor (Wang et al., 2011), a bio-memristor offering programmable dynamic loading (Hota et al., 2012), memory chips (Gogurla et al., 2013; Wang et al., 2016), or even sensor devices for applications in food industry (Zhu et al., 2016). Here, the sensors attach to the food to detect the local change of properties related to the food quality by wireless, passive antenna sensors (e.g., ripening of the banana by measuring chemical and physical changes notably ethylene emission, pathogenic bacterial contamination of cheese, spoilage of milk which increases the relative permittivity of the milk sample) (Tao et al., 2012). The implementation of silk-based electronics in medicine has been discussed as one of the most attractive fields of application, such as to detect *Staphilococcus aureus* infection or other bacteria by sticking of a graphene biosensor based on silk fibroin onto a tooth (Kim et al., 2009; Seo et al., 2018; Tao et al. 2012, 2014; Zhang et al., 1998; Zhu et al., 2016). Also the development of an impedimetric flexible biosensor based on a silk-conducting polymer for the detection of protein targets is discussed in literature (Xu and Yadavalli 2019). A further promising approach was recently introduced by Pal et al. by utilizing a biodegradable electrochemical sensor based on the conducting polymer silk for the detection of glucose, ascorbic acid and dopamine, respectively (Pal et al., 2016). The sensor showed reasonably good characteristics in terms of sensitivity with distinct drift behavior, however, only the working electrode has been fully biocompatible. In addition, in this experiment, the authors used a conventional standard Ag/AgCl reference electrode, which makes the application of the biosensor set-up for in-vivo and epidermal applications impossible.

The present study describes for the first time a fully biocompatible and degradable biosensor set-up consisting of a substrate fabricated from *Bombyx mori* silk fibroin. The substrate including the integrated electrodes is biodegradable. The biosensor was fabricated by combining thin- and thick-film technologies. In contrast to (Pal et al., 2016), the whole sensor set-up including the conducting tracks and parts of the contact wires have been further encapsulated with a biocompatible silicon rubber, promising full biocompatibility. The biosensor was electrochemically characterized by amperometric measurements with different glucose concentrations in phosphate buffer solution (PBS) and Ringer's solution (RS) which can be considered as substitute for physiological liquids such as blood plasma. Furthermore, potential stability of the Ag/AgCl quasi-reference electrode as well as bending stability of the flexible biosensor with regard to mechanical robustness were investigated. In addition, the cross-sensitivity to ascorbic acid, noradrenaline and adrenaline has been studied. Biocompatibility experiments according to DIN EN ISO 10993–5:2009-10 were carried out on silk fibroin membranes manufactured with and without thin-film platinum electrodes. Furthermore, degradation of silk fibroin membranes with thin-film platinum electrodes was assessed in a static test set-up.

2. Experimental

2.1. Materials

Glutaraldehyde, bovine serum albumin (BSA), glycerol, buffer components (monosodium phosphate and disodium phosphate), enzyme glucose oxidase (EC 1.4.4., from *Aspergillus niger*) and glucose monohydrate were purchased from Sigma-Aldrich (USA). Adrenaline solution (1 mg/mL) was bought from Infectopharm (Germany), noradrenaline (250 mg/mL) was obtained from Carinopharm (Germany) and ascorbic acid was ordered from Merck (Germany). Ringer's solution (8.6 g/L NaCl, 0.3 g/L KCl, 0.33 g/L $CaCl_2 \bullet 2H_2O$) was bought from Bernburg (Germany). ECOFLEX 0030 silicon rubber was bought from KauPo Plankenhorn e.K. (Germany). The two components of the silicon rubber were mixed in a 1:1 ratio and degassed for 3 min directly before using. Ag/AgCl paste was ordered from DuPont (United Kingdom). For the production of the fibroin substrate, silk cocoons (*Bombyx mori*) were used for protein extraction (Cantiere della Provvidenza, Italy). Glycerol and ethanol were purchased from VWR International (Belgium). Sodium carbonate was bought from AppliChem GmbH (Germany) and calcium chloride was bought from Merck KGaA (Germany). Cellulose membranes for dialysis were purchased from Spectrum Laboratories, Inc. (USA, MWCO: 3.5 kDa).

2.2. Preparation of fibroin substrate

To separate the glue-like sericin from the fibroin, the silk cocoons underwent a degumming process. An aqueous Na_2CO_3 solution (0.02 M) was produced, filled in a 10 L beaker glass and heated to 95–100 °C. 45 g of silk cocoons were added to the boiling solution and cooked and stirred constantly for 1 h. After boiling, the fibroin fibers were removed from the solution and rinsed with distilled water (ddH_2O). Afterwards, the fibers were placed in ddH_2O and left to swell for several minutes. The fibers were then further rinsed to remove all residuals. After washing, the fibers were loosened, plucked apart and laid out on a ventilation grid to dry for about 24 h at room temperature. In order to dissolve the degummed and dried fibroin wool, 3 g of fibers were added to 27 mL of a proprietary solvent based on Ajisawa's reagent. The mixture was stirred for 1 h at 75 °C. After the fibroin threads had dissolved completely, the intermediate was filtered through a filter paper and dialyzed against distilled water for 24 h at room temperature using tubular cellulose membranes to obtain the final protein solution (PureSilk®). The initial concentration of the resulting fibroin solution was 4% (w/v). The

solution was then stored at 4 °C. To obtain a flexible and stable fibroin film as substrate for the biosensor chip, glycerol and ethanol solution were added to the fibroin solution. The mixture had a volume percentage of fibroin solution of 50%, the ratio of glycerol to ethanol was 50:50 (v/v).

2.3. Fabrication of the biosensor structure

The fabrication process for the biosensor chip by combing thin- and thick-film technologies was separated in two parts, see Fig. 1 (a) and (d). For the preparation of the Pt working- and counter electrodes (Fig. 1 (b)), the fibroin solution was drop-casted on a silicon (Si) wafer as carrier. After drying for 24 h at 21 °C, the final fibroin substrate had a thickness of approximately 200 µm. The substrates were not subjected to any kind of post-treatment. The Pt working electrodes were deposited by means of thin-film technology under clean-room conditions. In brief, the first step consisted of electron-beam evaporation of an adhesion layer (20 nm titanium) and a 200 nm layer of platinum as electrode material via a shadow mask. The final wafer is shown in Fig. 1 (c) and was cut manually with a scalpel into 15 mm × 15 mm chips. Each sensor chip contains four platinum electrodes; two of them were used as counter electrodes, and two served as working electrode for the amperometric measurements.

For the glucose experiments, the enzyme membrane cocktail composition consisted of 20 µL glucose oxidase (GOX, 4 U/µL), 40 µL BSA (10%) and 40 µL glutaraldehyde (2%)/glycerol (10%). All individual reagents were freshly prepared before using and dissolved with phosphate buffer saline solution (PBS, 10 mM, pH 7.4). The final cocktail membrane was used with a volumetric ratio of the components: 1-2-2 (enzyme-BSA-glutaraldehyde/glycerol) (Molinnus et al., 2015). 4 µL of the mixed enzyme membrane cocktail with 3.2 U of GOX were drop-coated onto the platinum working electrode (diameter of 2 mm).

The Ag/AgCl quasi-reference electrode was prepared by thick-film technology, see Fig. 1 (d), (e). Again, the fibroin solution was drop-casted on a carrier, here a PTFE (polytetrafluoroethylene) support. The Ag/AgCl paste was screen-printed (screen-printer from Essemtec AG, Switzerland) onto the fibroin substrate via a stencil resulting in a thickness of approximately 20 µm of the Ag/AgCl layer. The final, printed fibroin substrate is shown in Fig. 1 (f), left. Before curing at a temperature of 60 °C for 2 h, the individual sensors were separated manually with a scalpel into 10 mm × 20 mm chips as described above. The final Ag/AgCl quasi-reference electrode is shown in Fig. 1 (f), right.

For both sensor parts, i) the fibroin substrate carrying the working/counter electrode and immobilized GOX, and ii) the Ag/AgCl reference electrode, connecting wires were glued onto the corresponding contact pads using a conductive silver lacquer (Ferrero GmbH, Germany). To enable biocompatibility for the whole biosensor chip, both parts were completely encapsulated back-to-back by a biocompatible silicon rubber (schematically shown in Fig. 1(a), (d)). This also defines the area of the Ag/AgCl reference electrode (diameter of 7 mm) and the size of the counter electrode (6.2 mm^2). Fig. 1(a) shows the encapsulated and connected biosensor chip with the top site of working/counter electrode, whereas Fig. 1(d) presents the same chip with the reference electrode on top (note, the biosensor chip is turned by 180°).

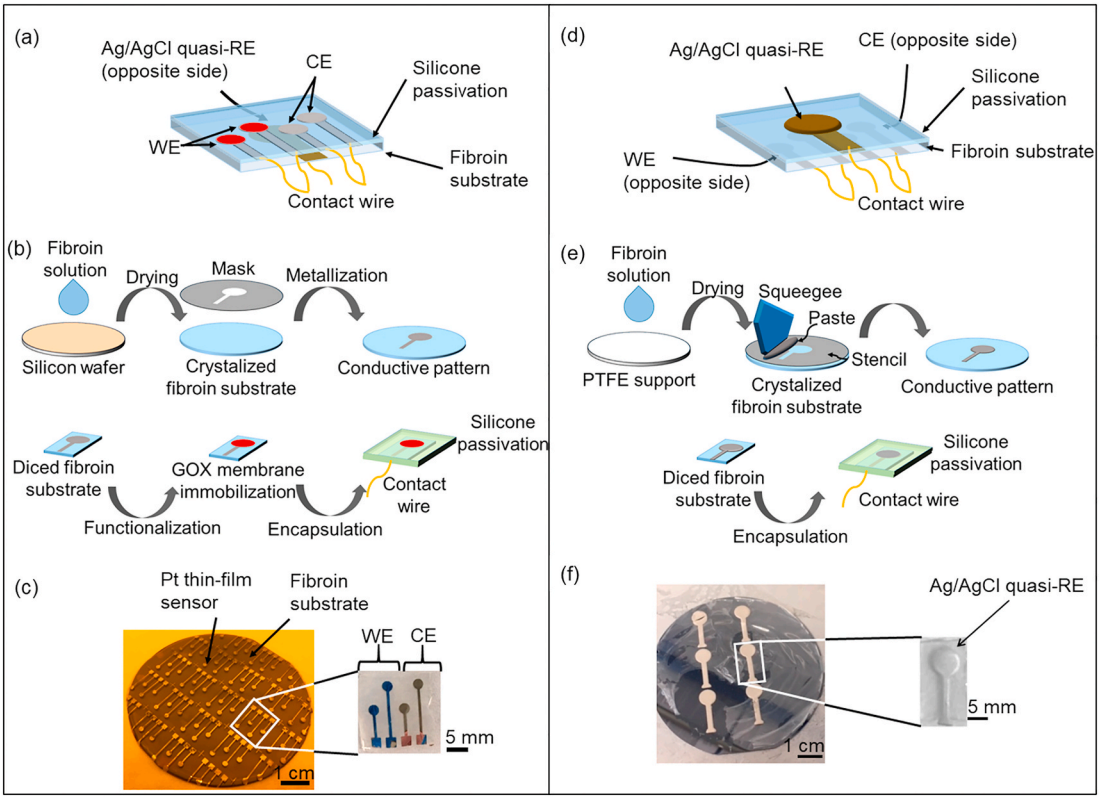

Fig. 1. (a) Schematic of the fabricated biocompatible glucose biosensor chip via thin- and thick-film technologies with Pt working- and counter electrodes on the upper side and Ag/AgCl quasi-reference electrode at the bottom; (b) fabrication steps of the Pt working- and counter electrodes by means of thin-film technology (schematically) and (c) light microscopic image of a 4-inch fibroin substrate with thin-film platinum electrodes (left) and diced chip carrying the final Pt working- and counter electrodes (right); (d) schematic of (a) about-faced with Ag/AgCl quasi-reference electrode on the upper site and Pt working- and counter electrodes on the bottom site; (e) fabrication steps of the Ag/AgCl quasi-reference electrode by means of thick-film technology (schematically) and (f) microscopic photo of 4-inch fibroin substrate with Ag/AgCl quasi-reference electrodes (left) and photo of the final Ag/AgCl quasi-reference electrode (right); GOX: glucose oxidase, RE: reference electrode, WE: working electrode, CE: counter electrode.

2.4. Measurement procedure

For the electrochemical characterization of the fibroin-based glucose biosensor, the experiments were carried out by connecting the sensor chip to a potentiostat (PalmSens, Palm Instruments BV, Netherlands). A three-electrode arrangement was used with the Pt working- and counter electrode, respectively, and the Ag/AgCl reference electrode. To determine the glucose concentration in the analyte, the resulting hydrogen peroxide from the enzymatic reaction is oxidized at a constant potential of +600 mV applied to the working electrode vs. the Ag/AgCl reference electrode; the generated current was recorded depending on time. The working potential was validated by linear-sweep voltammetry measurements in the diffusion-controlled plateau region. The sensitivity and long-term study of the fibroin-based biosensor chip was investigated in PBS, pH 7.4, at 21 °C under continuous stirring. Glucose concentrations from 0.5 mM to 3 mM were prepared from a stock solution of 250 mM glucose, which was stored at 4 °C. Each glucose concentration was measured for 10 min. For cross-sensitivity studies, 100 μM ascorbic acid, 50 nM noradrenaline, 50 nM adrenaline and different glucose concentrations (0.5 mM–3 mM) were used.

2.5. Degradation assessment procedure of fibroin substrate membranes

Degradation assessments were carried out underneath a laminar flow. First of all, PBS solution was produced by dissolving a single PBS tablet (PBS Tablets, Biotechnology Grade, VWR International, Radnor, USA) in 100 mL of distilled water by utilizing an autoclaved customary magnetic stirring plate. Each membrane was then sterilized underneath a customary UV-light and subsequently placed in a single chamber of a 12-well plate. 0.01 g of weighed protease-enzyme (protease from *Streptomyces griseus*, Type XIV, ≥3.5 U/mg solid powder, Sigma-Aldrich, St. Louis, USA) was then mixed in 10 mL PBS solution. Each well plate chamber was subsequently filled with enzyme solution until the respective membranes with Pt thin-film electrodes were entirely covered. The 12-well plate was then closed with its respective lid, cleaned with 70% ethanol from the outside and placed into an incubator (Heracell 150i CO_2 incubator, Thermo Scientific, Waltham, USA) at 37 °C. The well-plate was removed from the incubator at days 2, 4 and 10, respectively.

2.6. Cytocompatibility assessment procedure of fibroin substrate

Cytocompatibility experiments were carried out following the protocol of Jung et al. for indirect viability and cytotoxicity assays, additionally utilizing direct live dead stains on the respective fibroin substrate membranes (Jung et al., 2015). Detailed information about the procedure can be found in the Supplementary Information.

3. Results and discussion

3.1. Morphological characterization of platinum working electrode on the fibroin substrate

The prepared thin-film platinum electrode with silk fibroin from *Bombyx mori* as substrate was characterized by scanning electron microscopy (SEM, JEOL JSM-7800 F, Germany) applying an acceleration voltage of 5.0 kV. In Fig. 2, one can recognize a schematic of the Pt working electrode with the two regions that have been addressed in the SEM pictures (a), (b) and (c). Fig. 2 (a) shows the homogeneous deposition without any cracks of the thin-film platinum layer on top of the fibroin substrate. The platinum material has also been clearly identified by additional EDX measurements (energy-dispersive X-ray spectroscopy, JEOL JSM-7800 F, Germany, data not shown here). Remarkably, this dense deposition, even at higher magnification in Fig. 2 (b) and (c) in the cross-sectional views with the cut electrode structures, are well apparent. Note, the two different materials are clearly distinguishable from each other, see Fig. 2 (c).

3.2. Mechanical stress study of platinum working electrode on fibroin substrate and potential stability of Ag/AgCl quasi-reference electrode

Apart from its ability to reliably detect glucose levels, a biocompatible and flexible glucose biosensor should also possess long-term stability to withstand the rigors of daily users. Strain onto the flexible substrate with integrated electrodes can be caused by mechanical deformations, which can lead to adverse effects on the sensor performance.

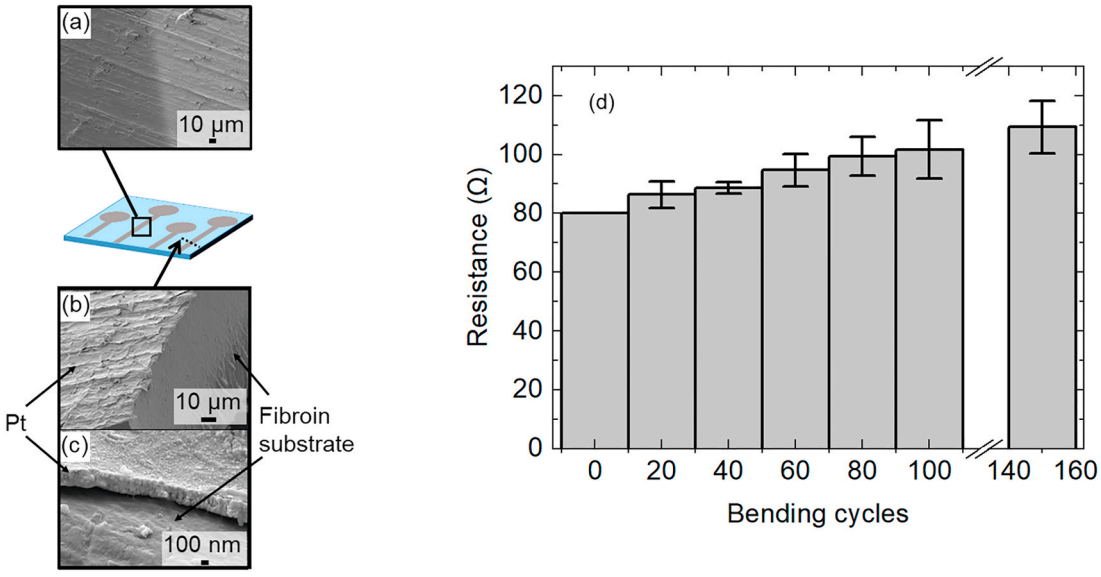

Fig. 2. SEM images of: (a) Pt working electrode on fibroin substrate at a magnification of 1,000x, (b) cross-sectional view of the interface Pt working electrode/fibroin substrate cut with a scalpel with Pt on top and fibroin as bulk material at a magnification of 950x, (c) a 200 nm Pt layer on top of the fibroin substrate (slight detachment due to mechanical stress by cutting, magnification of 30,000x). The schematic of the fabricated biocompatible biosensor chip is shown in the middle to illustrate the areas of interest for the SEM images. (d) Change in resistance of the platinum working electrode (N = 3 investigated sensor chips) after 160 bending cycles of the biocompatible, flexible fibroin substrate at 180°.

Therefore, the mechanical stability of the platinum electrode and related degradation has been investigated by repeatedly bending the substrate material for 180° by hand (for more details, see also Supplementary Information). The change of resistivity has been recorded by a conventional multimeter (Wavetek, USA) after 20, 40, 60 etc., up to 160 cycles. Fig. 2 (d) overviews that the resistance of the platinum working electrode is increasing from originally ~80 Ω–~115 Ω (N = 3 investigated sensors). Reasons for that might be small crack formations in the Pt layer. On the other hand, in spite of this resistance increase, the Pt working electrodes still work after 160 bending cycles with 180°, demonstrating that they can withstand repeated bending without losing functionality.

Additionally, the potential stability of the prepared Ag/AgCl quasi-reference electrode was studied against a commercial macroscopic Ag/AgCl reference electrode, see also publications (Bond and Lay 1986; Ghilane et al., 2006; Matsumoto et al., 2002; Ruch et al., 2009; Dico 2020; Gong et al., 2016). The results are shown in the Supplementary Information, where after 4 h a signal stability with a deviation of less than 500 μV was given.

3.3. Electrochemical characterization of biocompatible glucose sensor

The glucose sensitivity of the prepared biocompatible glucose biosensor chip was studied by amperometric measurements. Fig. 3 (a) and Fig. 3 (b) depict a typical dynamic response and corresponding calibration curve, respectively. The measurements were performed in PBS (pH 7.4), corresponding to the pH value in human blood. The biosensor responded instantaneously with distinct steps to varying glucose concentrations from 0.5 mM to 3 mM with a response time (T_{90}) of about 1 min. As expected, with increasing glucose concentration, the generated current is increasing due to the oxidation of H_2O_2. The corresponding calibration curve is shown in Fig. 3 (b), which is linear in the measured concentration range with a sensitivity of 0.2 ± 0.01 μA/mM. The experiment was repeated three times. A summary of the obtained results with the mean sensitivity and standard deviation is shown in the table of Fig. 3 (c). A mean glucose sensitivity of 0.24 ± 0.006 μA/mM could be achieved in the investigated concentration range measured by three individually prepared biosensors. The obtained results are comparable to data of recently published glucose biosensors, see e.g. (Liang et al., 2014; Pal et al., 2016), with biocompatible materials. However, in contrast to these described systems, in our biosensor chip not only the ‚sensor part' but also the reference electrode part as well as the encapsulation is manufactured of biocompatible components, yielding a bio-based and flexible electrochemical biosensor. Thus, the concept of this silk fiber-based strategy offers a new platform technology for application of further electrochemical biosensors.

Since the fibroin substrate is biodegradable only in the presence of proteolytic enzymes, the long-term stability of the fabricated glucose biosensor was proven for more than 100 days in an enzyme-free but moist environment. Between the measurements, the biosensor was stored at 4 °C. At each day, different glucose concentrations between 0.5 mM and 3 mM were examined.

Fig. 3 (d) depicts the mean values with the corresponding standard deviation shown as error bars of the obtained sensitivities of three individually fabricated biosensors. Within the first two days, the sensitivities of the sensors were stable between 0.20 μA/mM and 0.25 μA/mM, respectively. Within increasing measurement time, the average glucose sensitivity is decreasing and after 100 days, it is declining to a value of about 0.05 μA/mM. Several reasons might be responsible for this loss in sensitivity, i.e. i) the enzyme can be leached out of the membrane, ii) there is an activity loss of the enzyme, or iii) parts of the enzymatic membrane might be detached from the Pt working electrode.

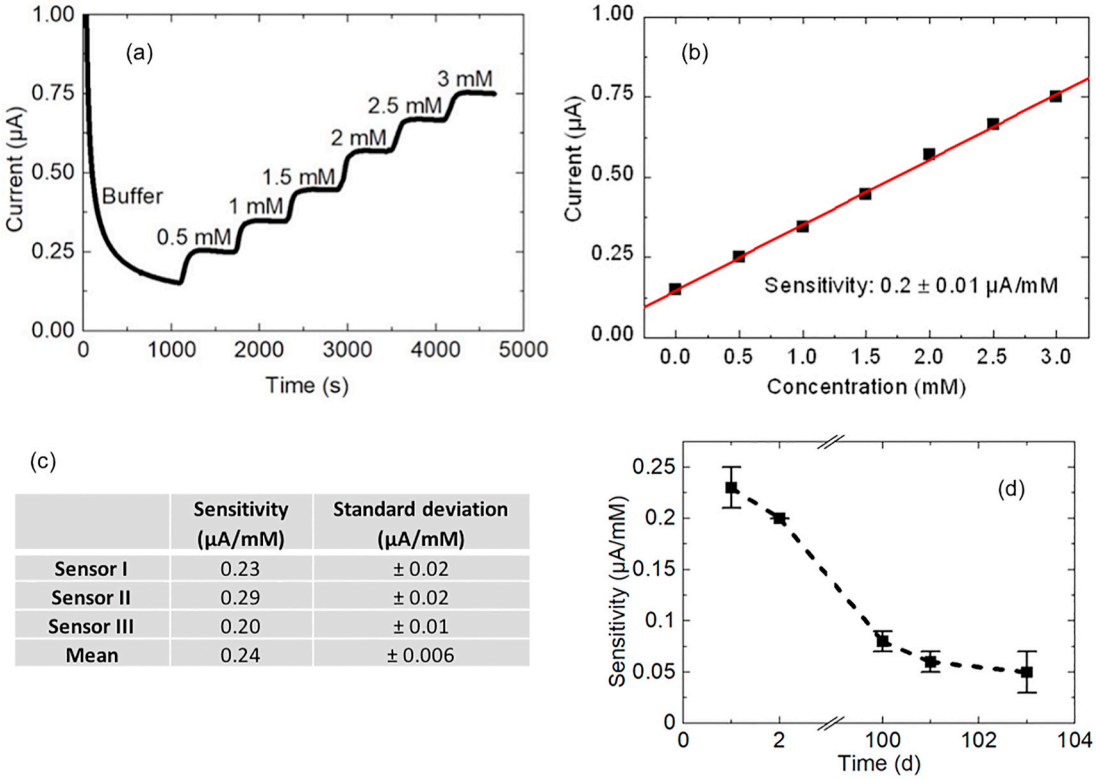

(c)

	Sensitivity (μA/mM)	Standard deviation (μA/mM)
Sensor I	0.23	± 0.02
Sensor II	0.29	± 0.02
Sensor III	0.20	± 0.01
Mean	0.24	± 0.006

Fig. 3. Representative dynamic response of the biocompatible glucose biosensor chip with immobilized GOX measured in PBS, pH 7.4, containing different glucose concentrations from 0.5 to 3 mM (a), and calibration curve of this biosensor (b). Summary of obtained sensitivities with standard deviation of three individual biosensors recorded in PBS with different glucose concentrations and calculated mean sensitivity with standard deviation (c). Lifetime study of the biocompatible glucose biosensor measured in a concentration range of 0.5 mM–3 mM in PBS (pH 7.4) over a measurement period of 103 days (d). Each data point consists of an average of three independently repeated measurements (N = 3).

Note, that the overall biosensor chip with biocompatible encapsulation is still running properly, in spite of the lowered glucose sensitivity, hence, proving its functionality. The obtained results were compared with state-of-the art technologies of implantable glucose biosensors. The overview can be found in the Supplementary Information (Table S1).

The manufactured flexible fibroin substrate has been proven to be completely insoluble and stable in direct contact with water (Silva et al., 2013). Only through the controlled addition of proteolytic enzymes the degradation and thus, the metabolization of the protein can be initiated. The degradation rate of the fibroin was already tested elsewhere, where the observed time-dependent weight loss indicated a progress in enzymatic degradation (Horan et al., 2005; Lu et al., 2011; Pritchard et al., 2011).

3.4. Study of cross-sensitivity of the biocompatible glucose biosensor and its application in Ringer's solution

The sensitivity of the amperometric glucose biosensor can be affected by inter alia, ascorbic acid, noradrenaline or adrenaline, which can be considered as most possible interfering compounds. Ascorbic acid, also known as Vitamin C, is a key element for the oxidation and reduction process in human organisms (Castro 2001). In human adults, the blood plasma concentration of ascorbic acid ranges from 20 μM to 110 μM (Baker et al., 1983; Scott et al., 1993). Adrenaline and noradrenaline belong to the group of catecholamines and are naturally present in blood. Their concentration in blood plasma is very low with ~0.3 nM and ~1.6 nM, respectively (Baba et al., 2013; Collste et al., 1986). Fig. 4 (a) exemplarily depicts the dynamic response of the biocompatible biosensor measured in PBS solution, while ascorbic acid with a concentration of 100 μM, noradrenaline of 50 nM and adrenaline of 50 nM were subsequently spiked to the buffer solution. Thereafter, different glucose concentrations between 0.5 mM and 3 mM were added into the same solution to verify the functionality of the prepared biosensor. This experiment clearly demonstrates that ascorbic acid, noradrenaline and adrenaline do not bring obvious interferences to the detection of different glucose concentrations; no significant contribution to a sensor signal change is recognizable. Furthermore, the sensitivity (0.26 ± 0.02 μA/mM) observed from the different glucose concentrations (0.5–3 mM), see Fig. 4 (b), is fully comparable with the measurements performed in pure buffer solution (see Fig. 3).

The prepared biosensor has been studied at physiological conditions in Ringer's solution at pH 7.4 (blood pH value), which contains similar electrolyte concentrations than in blood plasma. Fig. 4 (c) presents again glucose measurements in the concentration range between 0.5 mM and 3 mM. The glucose biosensor possesses a linear calibration characteristic with a mean sensitivity (N = 3) of 0.16 ± 0.01 μA/mM, evaluated from the calibration plot (Fig. 4 (d)). The slightly lower glucose sensitivity might be due to interferences from electrolyte compounds to the enzyme's activity. Nonetheless, the biocompatible glucose biosensor has been successfully validated in Ringer's solution at physiological conditions and therefore, shows great potential for future applications in real blood samples.

3.5. Degradation assessment of fibroin substrate membranes with thin-film platinum electrodes

Fibroin substrate membranes were almost thoroughly degraded by day 10 (see Fig. 5). The gross part of degradation took place between

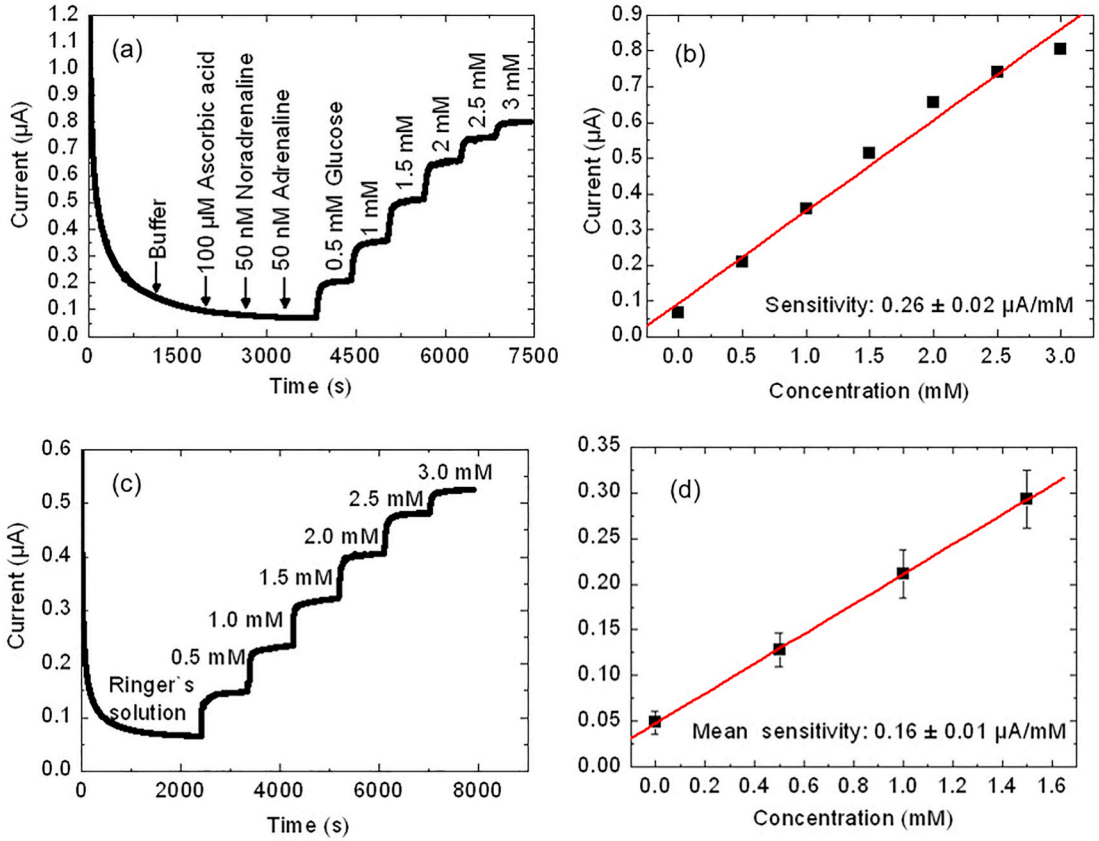

Fig. 4. Representative dynamic response of the biocompatible glucose biosensor measured in PBS (pH 7.4) proofing the cross-sensitivity by spiking sequentially 100 μM ascorbic acid, 50 nM noradrenaline, 50 nM adrenaline and different glucose concentrations in the range from 0.5 mM to 3 mM (a) to the buffer; corresponding calibration curve of this biosensor (b). Representative dynamic response of the biocompatible glucose biosensor chip with immobilized glucose oxidase measured in Ringer's solution, pH 7.4, containing different glucose concentrations from 0.5 to 3.0 mM (c) and corresponding calibration curve with standard deviation of three measured biosensors in the linear range between 0.5 and 1.5 mM (d).

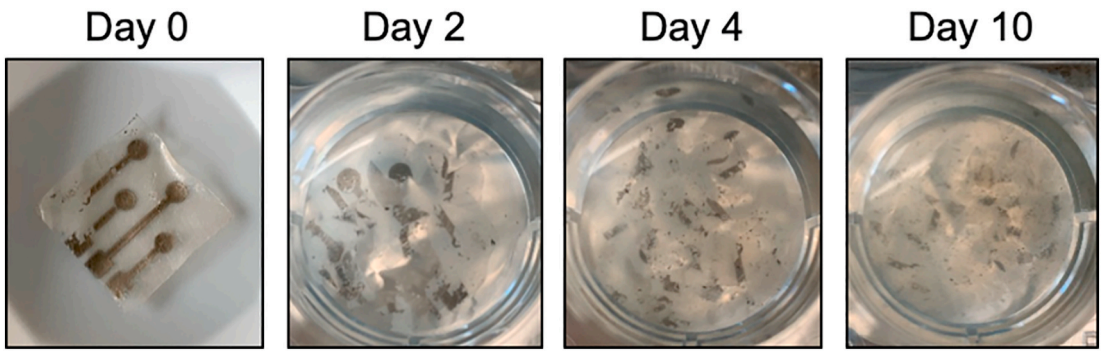

Fig. 5. Degradation assessment of fibroin substrate membranes with thin-film platinum electrodes. At day 2, disintegration with large particles is visible. At day 4, dust-like particles with few large particles indicate advancing degradation and at day 10, sole existence of dust-like particles indicate rather complete degradation.

days 0 and 2, as the platinum layer already exhibited pronounced disintegration at day 2 with few large particles being visible within the chamber. At day 4, sole visibility of dust-like platinum particles with few large particles indicated almost thorough fibroin substrate membrane degradation, whereas at day 10, fairly complete degradation was observed.

3.6. Cytocompatibility assessment of fibroin substrate membranes with and without thin-film platinum electrodes

In order to assess biocompatibility of the fibroin substrate membranes, with and without thin-film platinum electrodes, different cell culture-based tests were conducted. To evaluate the effects of the dissolving material (i.e., the degradation byproducts) as well as the influence of potentially liberated impurities, indirect testing was conducted on the extracts derived from the different material groups. BrdU detects the quantity of 5-bromo-2′-deoxyuridine (BrdU) incorporated into cellular DNA during cell proliferation using an anti-BrdU antibody, while XTT quantifies cellular metabolic activity via colorimetric assay of added, extracellular tetrazolium salts, which are transformed into colored formazan derivatives via mitochondrial dehydrogenase. With regard to the BrdU assay, all groups, namely the extracts derived from

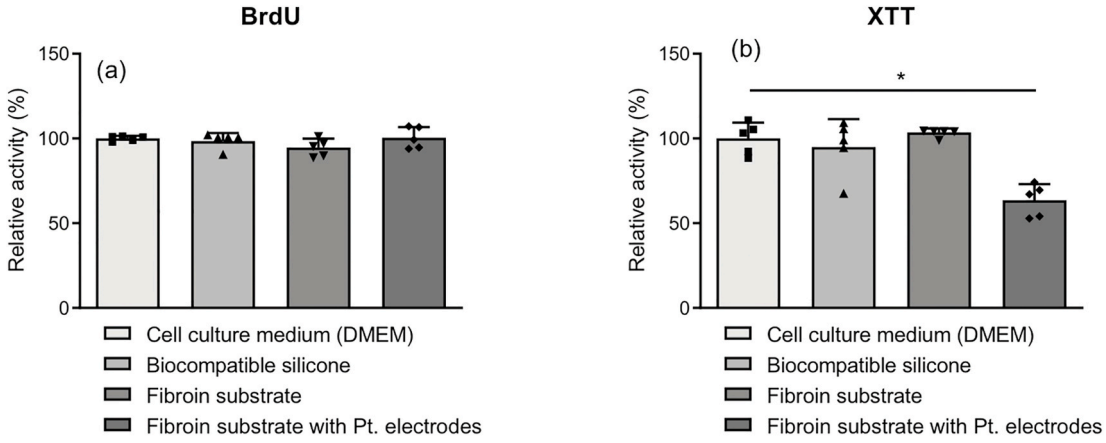

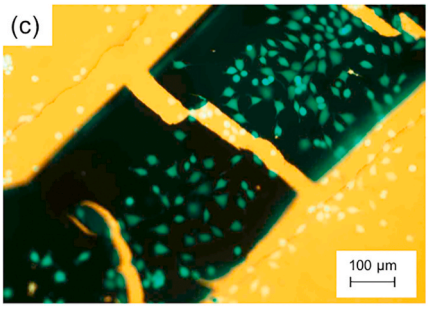

Fig. 6. (a) Results of extract-based cell culture assay BrdU on fibroin substrate membranes with and without thin-film platinum electrodes. All groups exhibited similar absorbance values, indicating cell proliferation at approx. 100% and therefore suggesting thorough cytocompatibility of all tested materials. (b) Results of extract-based cell culture assay XTT on fibroin substrate membranes with and without thin-film platinum electrodes. All groups except fibroin substrate membranes with thin-film platinum electrodes exhibited similar absorbance values, indicating cell metabolic activity at approx. 100% and therefore suggesting thorough cytocompatibility of all named tested materials. Fibroin substrates with platinum electrodes barely reached the DIN EN ISO 10993–5:2009-10 defined 70% threshold, therefore indicating decreased cell metabolic activity and forwarding cytotoxic potential. (c) Live dead stain of L-929 mouse fibroblasts on fibroin substrate membranes with thin-film platinum electrodes (cells were incubated for 24 h on the test material). Note the abundance of green, spindle-shaped, vital cells and the absence of roundly shaped red cells, thus proposing rather pronounced biocompatibility with absent cytotoxicity. (For interpretation of the references to color in this figure legend, the reader is referred to the Web version of this article.)

the fibroin substrate membranes with and without thin-film platinum electrodes, the biocompatible silicone and the extract composed of regular cell culture medium expressed similar absorbance values, hereby indicating similar levels of cellular metabolic activity at approx. 100%. Thus, no cytotoxic potential could be proven for any of the groups (see Fig. 6 (a)).

The XTT assay exhibited equivalently elevated absorbance values concerning fibroin substrate membranes without thin-film platinum electrodes, the biocompatible silicone and the extract composed of regular cell culture medium, therefore indicating adequate cellular metabolic activity at approx. 100%. Thus, for these groups, no cytotoxic potential could be proven either (see Fig. 6 (b)). In contrast to the BrdU assay, fibroin substrate membranes with thin-film platinum electrodes exhibited significantly lower absorbance values within the XTT assay in comparison to the other groups, hereby indicating reduced cellular metabolic activity and potential cytotoxicity. In summary, fibroin substrate membranes without thin-film platinum electrodes showed comparably elevated absorbance values indicating adequate metabolic activity and cellular proliferation throughout both tests with absorbance values clearly exceeding the 70% threshold defined by the DIN EN ISO 10993–5:2009-10 standard (Beuth Verlag GmbH), hereby indicating biocompatibility. Whereas, the fibroin substrate membranes with thin-film platinum electrodes barely reached the aforementioned threshold within the XTT assay, but performed equal to the other groups within the BrdU assay. Hence, within this study, cytotoxic potential based on indirect testing of extracts is not present for fibroin substrate membranes without thin-film platinum electrodes. BrdU and XTT assays yielded different results for fibroin substrate membranes with thin-film platinum electrodes.

Thus, in order to obtain a more complete picture of the biological interaction of fibroin substrate membranes with and without thin-film platinum electrodes, complementary direct testing by live dead stains was performed. In comparison to the indirect testing of extracts, the direct seeding of fibroblast cells onto the surface of aforementioned fibroin substrate membranes with thin-film platinum electrodes with consecutive detection of either red fluorescing DNA dye PI, which cannot enter intact healthy cells due to its polar nature, or green-emitting dye, being only present in viable cells, gives a more complete view on the immediate cytotoxic potential of the material. This additionally considers the physico-chemical interaction straight at the materials surface. Fig. 6 (c) shows the overlay of green- and red-emitting stains. While an abundant amount of viable green cells can be observed, no dead red-stained cells can be found on the fibroin substrate membranes with thin-film platinum electrodes. Notably, there is a clear tendency of cells residing on the respective platinum electrode. The adherent cells appear clustered and spindle-shaped, hereby indicating cell vitality. The absence of roundly shaped cells further undermines the absence of cytotoxicity of the fibroin substrate membranes with thin-film platinum electrodes. In sum, fibroin substrate membranes with thin-film platinum electrodes display acceptable cell interaction with low cytotoxic potential expressed via direct cell culture testing. This is further supported by the indirect BrdU assay and remains in contrast to the XTT assay.

4. Conclusions

This study describes the fabrication of a flexible biocompatible glucose biosensor chip by combining thin- and thick-film technologies based on silk fibroin from *Bombyx mori* fiber as a natural substrate to replace artificial materials. To ensure biocompatibility of the whole biosensor chip (also including reference- and counter electrode), the conducting tracks as well as the connecting wires were encapsulated with a biocompatible silicone rubber. The biosensor chip was characterized regarding its morphological structure, mechanical robustness and electrochemical properties. Glucose concentrations in the biomedically relevant concentration range from 0.5 mM to 3 mM were detected in buffer solution at physiological pH of 7.4. Cross-sensitivity studies did not find interfering signals from ascorbic acid, noradrenaline or adrenaline compared with the response to different glucose concentrations. However, the sensitivity of the glucose biosensor might be also affected by other components such as amino acids or carbohydrates. One future strategy could be the implementation of an additional perm-selective membrane (molecular size) that favours glucose diffusion to the enzyme. The glucose biosensor successfully performed measurements in Ringer's solution, the next step is now, to proof the sensor behavior in biological liquids such as blood. Degradation assessment of fibroin substrate membranes with thin-film platinum electrodes demonstrated, that the vast majority of degradation takes place within the first two days and the electrodes were almost entirely degraded at day 10. In future experiments, the biocompatible silicone encapsulation shall be replaced by a fully biodegradable biopolymer such as polycaprolactone (PCL). Indirect biocompatibility evaluation of fibroin substrate membranes with and without thin-film platinum electrodes was performed according to the DIN EN ISO 10993–5:2009-10 standard for cytotoxicity. Fibroin substrate membranes without thin-film platinum electrodes did not yield any cytotoxic potential, whereas fibroin substrate membranes with thin-film platinum electrodes exhibited cytotoxic potential in the XTT assay, but not in the BrdU assay. Direct cell culture on the fibroin substrate membranes with thin-film platinum electrodes yielded highly satisfactory results, showing an abundancy of green-stained, vital cells on the material surface. This finding lies in accordance with the performed BrdU assay. Therefore, the incorporation of platinum within the membranes may have interfered with the XTT assay, as the recorded results deviated from the previously mentioned. We therefore assume that fibroin substrate membranes with thin-film platinum electrodes exhibit similar biocompatible properties as the other investigated groups.

Casted silk fibroin substrates are highly interesting due to their unique properties such as optical transparency, flexibility, permeability, biocompatibility and biodegradability (Acharya et al., 2008; Kopp et al., 2020; Minoura et al., 1995). The ability to manage the structure and morphology of regenerated silk fibroin through various processing methods has expanded its widespread use in clinical applications. In addition, to raise the potential of silk fibroin as a new medical material and to ensure biocompatibility we avoided toxic, cost-intensive and harmful agents, like lithium bromide and produced substrates based only on aqueous solution.

One future major challenge for those biocompatible, flexible biosensors for biomedical applications is their non-inflammatory contact with human tissue e.g., when used for wounds or implantable monitoring devices. Silk fibroin can be utilized for mastering this hurdle. It has already been proven that casted fibroin films ensure safe and effective wound healing in animal models and in randomized, clinical trials (Zhang et al., 2017). Further, it inhibits bacterial infections and offers adjustable biodegradability. To extend the remarkable properties of fibroin films, one scenario might be an enzyme-triggered, timely defined degradation (and therewith dissolution) of the whole biosensor for in-vivo or epidermal point-of-care applications, or even serving as drug-release actuator. Another major role might play the process optimization of the casted fibroin, to find the ideal balance between mechanical and biological properties but at the same time to ensure stable sensor performance. For this purpose, tunable surface conditions of the fibroin film and adapted or alternative manufacturing methods should be considered.

CRediT authorship contribution statement

Denise Molinnus: Conceptualization, Validation, Formal analysis, Investigation, Writing – original draft, Project administration. **Aleksander Drinic:** Validation, Formal analysis, Investigation, Writing – original draft. **Heiko Iken:** Validation, Investigation. **Nadja Kröger:** Formal analysis, Investigation, writing. **Max Zinser:** Validation, review

& editing. **Ralf Smeets:** Validation, review & editing. **Marius Köpf:** Conceptualization, Writing – review & editing, Supervision, Project administration. **Alexander Kopp:** Validation, Writing – review & editing. **Michael J. Schöning:** Conceptualization, Validation, Writing – review & editing, Supervision, Project administration.

Declaration of competing interest

The authors declare that they have no known competing financial interests or personal relationships that could have appeared to influence the work reported in this paper.

Acknowledgement

The authors thank D. Rolka for the SEM and EDX images and S. Fuest and A. Baranowsky for support on the biological testing as well as valuable discussions. Also many thanks to J. Kiesel and S. Woege for their assisting during the electrochemical measurements.

Appendix A. Supplementary data

Supplementary data to this article can be found online at https://doi.org/10.1016/j.bios.2021.113204.

References

Acharya, C., Ghosh, S.K., Kundu, S.C., 2008. J. Mater. Sci. Mater. Med. 19 (8), 2827–2836.
Anderson, J.M., 2001. Annu. Rev. Mater. Res. 31 (1), 81–110.
Anderson, J.M., Langone, J.J., 1999. J. Contr. Release 57 (2), 107–113.
Anderson, J.M., Rodriguez, A., Chang, D.T., 2008. Semin. Immunol. 20 (2), 86–100.
Arai, T., Freddi, G., Innocenti, R., Tsukada, M., 2004. J. Appl. Polym. Sci. 91 (4), 2383–2390.
Arifuzzaman, M., Millhouse, P.W., Raval, Y., Pace, T.B., Behrend, C.J., Beladi Behbahani, S., DesJardins, J.D., Tzeng, T.-R.J., Anker, J.N., 2019. Analyst 144 (9), 2984–2993.
Baba, Y., Nakajo, M., Hayashi, S., 2013. Endocrine 43 (1), 219–224.
Baker, J.K., Kapeghian, J., Verlangieri, A., 1983. J. Liq. Chromatogr. Relat. Technol. 6 (7), 1319–1332.
Bond, A.M., Lay, P.A., 1986. J. Electroanal. Chem. 199 (2), 285–295.
Cadée, J.A., Brouwer, L.A., Otter, W. den, Hennink, W.E., van Luyn, M.J.A., 2001. J. Biomed. Mater. Res. 56 (4), 600–609.
Cao, Y., Wang, B., 2009. Int. J. Mol. Sci. 10 (4), 1514–1524.
Castro, S., 2001. Talanta 55 (2), 249–254.
Chen, F., Porter, D., Vollrath, F., 2012. Acta Biomater. 8 (7), 2620–2627.
Collste, P., Brismar, B., Alveryd, A., Björkhem, I., Hårdstedt, C., Svensson, L., Ostman, J., 1986. Acta Chir. Scand. Suppl. 530, 67–71.
Dico, 2020. Silber-Silberchlorid-Pasten - Dico Electronic GmbH accessed. https://www.dico-electronic.de/silber-silberchlorid-pasten.html. (Accessed 23 November 2020).
Fournier, E., Passirani, C., Montero-Menei, C.N., Benoit, J.P., 2003. Biomaterials 24 (19), 3311–3331.
Frost, M.C., Meyerhoff, M.E., 2002. Curr. Opin. Chem. Biol. 6 (5), 633–641.
Fujioka, K., 1998. Adv. Drug Deliv. Rev. 31 (3), 247–266.
Geiger, M., Li, R.H., Friess, W., 2003. Adv. Drug Deliv. Rev. 55 (12), 1613–1629.
Ghilane, J., Hapiot, P., Bard, A.J., 2006. Anal. Chem. 78 (19), 6868–6872.
Gogurla, N., Mondal, S.P., Sinha, A.K., Katiyar, A.K., Banerjee, W., Kundu, S.C., Ray, S.K., 2013. Nanotechnology 24 (34), 345202.
Gong, C.-S.A., Syu, W.-J., Lei, K.F., Hwang, Y.-S., 2016. Sensors 16 (10).
Horan, R.L., Antle, K., Collette, A.L., Wang, Y., Huang, J., Moreau, J.E., Volloch, V., Kaplan, D.L., Altman, G.H., 2005. Biomaterials 26 (17), 3385–3393.
Hota, M.K., Bera, M.K., Kundu, B., Kundu, S.C., Maiti, C.K., 2012. Adv. Funct. Mater. 22 (21), 4493–4499.
Humenik, M., Scheibel, T., Smith, A., 2011. Prog. Mol. Biol. Transl. Sci. 103, 131–185.
Irimia-Vladu, M., 2014. Chem. Soc. Rev. 43 (2), 588–610.
Jung, O., Smeets, R., Porchetta, D., Kopp, A., Ptock, C., Müller, U., Heiland, M., Schwade, M., Behr, B., Kröger, N., Kluwe, L., Hanken, H., Hartjen, P., 2015. Acta Biomater. 23, 354–363.
Kang, T., Lee, I., Oh, S., Jang, T., Kim, Y., Ahn, H., Kim, G., Shin, S.-U., Jeong, S., Sylvester, D., Blaauw, D., 2019. A 1.74.12 mm 3 fully integrated pH sensor for implantable applications using differential sensing and drift-compensation. In: 2019 Symposium on VLSI Circuits Digest of Technical Papers. IEEE, Piscataway, NJ, USA, pp. C310–C311. June 9-14, 2019, Kyōto, Japan.
Kifle, Y., Wikner, J.J., Zotterman, J., Ryden, L., Farnebo, S., 2019. Annu. Int. Conf. IEEE Eng. Med. Biol. Soc. 2019, 4359–4362.
Kim, D.-H., Kim, Y.-S., Amsden, J., Panilaitis, B., Kaplan, D.L., Omenetto, F.G., Zakin, M. R., Rogers, J.A., 2009. Appl. Phys. Lett. 95 (13), 133701.
Kopp, A., Smeets, R., Gosau, M., Friedrich, R.E., Fuest, S., Behbahani, M., Barbeck, M., Rutkowski, R., Burg, S., Kluwe, L., Henningsen, A., 2019. In Vivo 33 (3), 757–762.
Kopp, A., Smeets, R., Gosau, M., Kröger, N., Fuest, S., Köpf, M., Kruse, M., Krieger, J., Rutkowski, R., Henningsen, A., Burg, S., 2020. Bioact. Mater. 5 (2), 241–252.
Liang, B., Fang, L., Hu, Y., Yang, G., Zhu, Q., Ye, X., 2014. Nanoscale 6 (8), 4264–4274.
Lu, Q., Zhang, B., Li, M., Zuo, B., Kaplan, D.L., Huang, Y., Zhu, H., 2011. Biomacromolecules 12 (4), 1080–1086.
Lucas, F., Shaw, J.T., Smith, S.G., 1957. Biochem. J. 66 (3), 468–479.
Lunsford, L., McKeever, U., Eckstein, V., Hedley, M.L., 2000. J. Drug Target. 8 (1), 39–50.
Maruoka, S., Matsuura, T., Kawasaki, K., Okamoto, M., Yoshiaki, H., Kodama, M., Sugiyama, M., Annaka, M., 2006. Curr. Eye Res. 31 (7–8), 599–606.
Matsumoto, T., Ohashi, A., Ito, N., 2002. Anal. Chim. Acta 462 (2), 253–259.
Minoura, N., Aiba, S., Gotoh, Y., Tsukada, M., Imai, Y., 1995. J. Biomed. Mater. Res. 29 (10), 1215–1221.
Molinnus, D., Bäcker, M., Iken, H., Poghossian, A., Keusgen, M., Schöning, M.J., 2015. Phys. Status Solidi A 212 (6), 1382–1388.
Nouira, W., Haddad, R., Barhoumi, H., Maaref, A., Bausells, J., Bessueille, F., Léonard, D., Jaffrezic-Renault, N., Errachid, A., 2009. Sens. Lett. 7 (5), 689–693.
Oka, M., Ushio, K., Kumar, P., Ikeuchi, K., Hyon, S.H., Nakamura, T., Fujita, H., 2000. Proc. Inst. Mech. Eng. H 214 (1), 59–68.
Onuki, Y., Bhardwaj, U., Papadimitrakopoulos, F., Burgess, D.J., 2008. J. Diabetes Sci. Technol. 2 (6), 1003–1015.
Pal, R.K., Farghaly, A.A., Wang, C., Collinson, M.M., Kundu, S.C., Yadavalli, V.K., 2016. Biosens. Bioelectron. 81, 294–302.
Paradossi, G., Cavalieri, F., Chiessi, E., Spagnoli, C., Cowman, M.K., 2003. J. Mater. Sci. Mater. Med. 14 (8), 687–691.
Pickup, J.C., Shaw, G.W., Claremont, D.J., 1987. Biosensors 3 (6), 335–346.
Porter, D., Vollrath, F., 2009. Adv. Mater. 21 (4), 487–492.
Pritchard, E.M., Valentin, T., Boison, D., Kaplan, D.L., 2011. Biomaterials 32 (3), 909–918.
Quinn, C.A., Connor, R.E., Heller, A., 1997. Biomaterials 18 (24), 1665–1670.
Rivnay, J., Owens, R.M., Malliaras, G.G., 2014. Chem. Mater. 26 (1), 679–685.
Rockwood, D.N., Preda, R.C., Yücel, T., Wang, X., Lovett, M.L., Kaplan, D.L., 2011. Nat. Protoc. 6 (10), 1612–1631.
Ruch, P.W., Cericola, D., Hahn, M., Kötz, R., Wokaun, A., 2009. J. Electroanal. Chem. 636 (1–2), 128–131.
Sajid, M., Aziz, S., Kim, G.B., Kim, S.W., Jo, J., Choi, K.H., 2016. Sci. Rep. 6 (1), 30065.
Scott, P., Bruce, C., Schofield, D., Shiel, N., Braganza, J.M., McCloy, R.F., 1993. Br. J. Surg. 80 (6), 750–754.
Seo, J.-W., Kim, H., Kim, K., Choi, S.Q., Lee, H.J., 2018. Adv. Funct. Mater. 28 (36), 1800802.
Seves, A., Romanò, M., Maifreni, T., Sora, S., Ciferri, O., 1998. Int. Biodeterior. Biodegrad. 42 (4), 203–211.
Sierra-Montes, J.M., Pereira-Simon, S., Smail, S.S., Herrera, R.J., 2005. Gene 352, 127–136.
Silva, M.F., Moraes, M.A. de, Nogueira, G.M., Rodas, A.C.D., Higa, O.Z., Beppu, M.M., 2013. J. Appl. Polym. Sci. 128 (1), 115–122.
Tao, H., Brenckle, M.A., Yang, M., Zhang, J., Liu, M., Siebert, S.M., Averitt, R.D., Mannoor, M.S., McAlpine, M.C., Rogers, J.A., Kaplan, D.L., Omenetto, F.G., 2012. Adv. Mater. 24 (8), 1067–1072.
Tao, H., Hwang, S.-W., Marelli, B., An, B., Moreau, J.E., Yang, M., Brenckle, M.A., Kim, S., Kaplan, D.L., Rogers, J.A., Omenetto, F.G., 2014. Proc. Natl. Acad. Sci. U.S. A. 111 (49), 17385–17389.
Ude, A.U., Eshkoor, R.A., Zulkifili, R., Ariffin, A.K., Dzuraidah, A.W., Azhari, C.H., 2014. Mater. Des. 57, 298–305.
Vallejo-Heligon, S.G., Brown, N.L., Reichert, W.M., Klitzman, B., 2016. Acta Biomater. 30, 106–115.
Vepari, C., Kaplan, D.L., 2007. Prog. Polym. Sci. 32 (8–9), 991–1007.
Vercruysse, K.P., Prestwich, G.D., 1998. Crit. Rev. Ther. Drug Carrier Syst. 15 (5), 513–555.
Beuth Verlag GmbH. DIN EN ISO 10993-5:2009-10, Biologische Beurteilung von Medizinprodukten_- Teil_5: Prüfungen auf In-vitro-Zytotoxizität (ISO_10993-5: 2009); Deutsche Fassung EN_ISO_10993-5:2009. Beuth Verlag GmbH, Berlin..
Vos, P. de, Hoogmoed, C.G., Busscher, H.J., 2002. J. Biomed. Mater. Res. 60 (2), 252–259.
Wang, C.-H., Hsieh, C.-Y., Hwang, J.-C., 2011. Adv. Mater. 23 (14), 1630–1634.
Wang, Y., Vaddiraju, S., Gu, B., Papadimitrakopoulos, F., Burgess, D.J., 2015. J. Diabetes Sci. Technol. 9 (5), 966–977.
Wang, H., Zhu, B., Wang, H., Ma, X., Hao, Y., Chen, X., 2016. Small 12 (25), 3360–3365.
Wang, L., Luo, Z., Zhang, Q., Guan, Y., Cai, J., You, R., Li, X., 2019. Fibers Polym. 20 (1), 45–50.
Weir, R.F., Troyk, P.R., DeMichele, G.A., Kerns, D.A., Schorsch, J.F., Maas, H., 2009. IEEE Trans. Biomed. Eng. 56 (1), 159–171.
Xu, M., Yadavalli, V.K., 2019. ACS Sens. 4 (4), 1040–1047.
Zhang, Y.-Q., Shen, W.-D., Gu, R.-A., Zhu, J., Xue, R.-Y., 1998. Anal. Chim. Acta 369 (1–2), 123–128.
Zhang, H., Magoshi, J., Becker, M., Chen, J.Y., Matsunaga, R., 2002. J. Appl. Polym. Sci. 86 (8), 1817–1820.
Zhang, W., Chen, L., Chen, J., Wang, L., Gui, X., Ran, J., Xu, G., Zhao, H., Zeng, M., Ji, J., Qian, L., Zhou, J., Ouyang, H., Zou, X., 2017. Adv. Healthc. Mater. 6 (10).
Zhu, B., Wang, H., Leow, W.R., Cai, Y., Loh, X.J., Han, M.-Y., Chen, X., 2016. Adv. Mater. 28 (22), 4250–4265.